Article

Combined Quantum Mechanics/Molecular Mechanics Study on the Reversible Isomerization of Glucose and Fructose Catalyzed by *Pyrococcus furiosus* Phosphoglucose Isomerase

Ruibo Wu, Hujun Xie, Zexing Cao, and Yirong Mo

J. Am. Chem. Soc., **2008**, 130 (22), 7022-7031 • DOI: 10.1021/ja710633c • Publication Date (Web): 10 May 2008

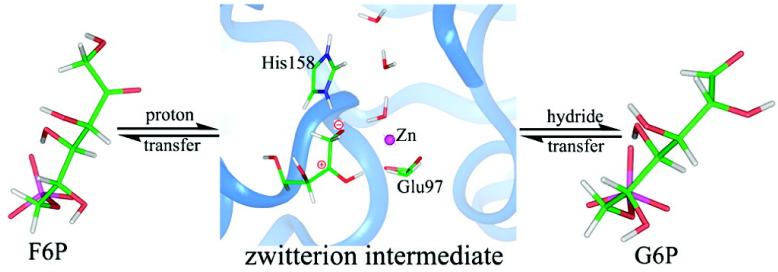

More About This Article

Additional resources and features associated with this article are available within the HTML version:

- Supporting Information
- Access to high resolution figures
- Links to articles and content related to this article
- Copyright permission to reproduce figures and/or text from this article

View the Full Text HTML

J|A|C|S
ARTICLES

Published on Web 05/10/2008

Combined Quantum Mechanics/Molecular Mechanics Study on the Reversible Isomerization of Glucose and Fructose Catalyzed by *Pyrococcus furiosus* Phosphoglucose Isomerase

Ruibo Wu,[†] Hujun Xie,[†] Zexing Cao,[*,†] and Yirong Mo[†,‡]

Department of Chemistry and State Key Laboratory of Physical Chemistry of Solid Surfaces, Xiamen University, Xiamen, 361005, China, and Department of Chemistry, Western Michigan University, Kalamazoo, Michigan 49008

Received November 27, 2007; E-mail: zxcao@xmu.edu.cn

Abstract: Phosphoglucose isomerase (PGI), which catalyzes the reversible interconversion of glucose 6-phosphate (G6P) and fructose 6-phosphate (F6P), is represented by two evolutionarily distinct protein families. One is a conventional type in eubacteria, eukaryotes, and a few archaea, where the active sites contain no metal ions and reactions proceed via the *cis*-enediol intermediate mechanism. The second type, found recently in euryarchaeota species, belongs to metalloenzymes, and controversies exist over whether the catalyzed isomerization occurs via the *cis*-enediol intermediate mechanism or a hydride shift mechanism. We studied the reversible interconversion of the open-chain form G6P and F6P catalyzed by the metal-containing *Pyrococcus furiosus* PGI by performing QM(B3LYP)/MM single-point optimizations and QM(PM3)/MM molecular dynamics simulations. A zwitterion intermediate-based mechanism, which involves both proton and hydride transfers, has been put forward. The presence of the key zwitterionic intermediate in this mechanism can effectively reconcile the controversial mechanisms and rationalize the enzymatic reaction. Computations show that the overall isomerization process is quite facile, both dynamically and thermodynamically. The crucial roles of conserved residues have been elucidated on the basis of computations on their alanine mutants. In particular, Tyr152 pushes the H1 transfer through a hydride-shift mechanism and dominates the stereochemistry selectivity of the hydrogen transfer. The rest of the conserved residues basically maintain the substrate in the near-attack reactive conformation and mediate the proton transfer. Although Zn^{2+} is not directly involved in the reaction, the metal ion as a structural anchor constructs a hydrogen bond wire to connect the substrate to the outer region, providing a potential channel for hydrogen exchange between the substrate and solvent.

Introduction

Phosphoglucose isomerase (PGI) is a dimeric cytosolic enzyme responsible for the second step of glycolysis in most higher organisms and thus is involved in glucogenesis via the Embden−Meyerhof pathway by catalyzing the reversible isomerization of glucose-6-phosphate (G6P), an aldose, to fructose-6-phosphate (F6P), a ketose (Scheme 1).[1–4] The bifunctional phosphoglucose/phosphomannose isomerase (PGI/PMI) family and the PGI family form a PGI superfamily, the members of which play a critical role in sugar metabolism of eukarya, bacteria, and some archaea. Remarkably, PGI is a moonlighting protein with four unique functions inside and outside cells.[5,6] Apart from functioning as an isomerase, PGI also serves as a neuroleukin, an autocrine motility factor, and a differentiation and maturation mediator.[7] Extensive mechanistic studies have been conducted to elucidate the enzymatic catalysis.[2,3,8–11] For instance, early work suggested that, in the isomerization of G6P to F6P, there is an intramolecular proton transfer, rather than a hydride transfer, between C1 and C2 with partial exchange of the proton of the substrate with protons derived from the medium.[2,3] Significantly, Seeholzer proposed a mechanism showing the relationship between the isomerase, anomerase, and epimerase activities of PGI.[8] However, further elucidation at the atomic level was derived from the recent high-resolution crystal structures.[6,12–21] Analyses of the structures of PGI enzymes complexed with or without inhibitors have established

[†] Xiamen University.
[‡] Western Michigan University.

(1) Lohman, K. *Biochem. Z.* **1933**, *262*, 137. Parr, C. W. *Nature* **1956**, *178*, 1401.
(2) Topper, Y. J. *J. Biol. Chem.* **1957**, *225*, 419.
(3) Rose, I. A.; O'Connell, E. L. *J. Biol. Chem.* **1961**, *236*, 3086.
(4) Rose, I. A. *Mechanism of the Aldose−Ketose Isomerase Reactions*; John Wiley & Sons: New York, 1975; Vol. 43.
(5) Jeffery, C. J. *Trends Biochem. Sci.* **1999**, *24*, 8. Copley, S. D. *Curr. Opin. Chem. Biol.* **2003**, *7*, 265.
(6) Jeffery, C. J.; Brian, J. B.; Wade, C.; Tagmer, R.; Gregory, A. P. *Biochemistry* **2000**, *39*, 955.
(7) Chaput, M.; Claes, V.; Portetelle, D.; Cludts, I.; Cravador, A.; Burny, A.; Gras, H.; Tartar, A. *Nature* **1988**, *332*, 454. Faik, P.; Walker, J. I.; Redmill, A. A.; Morgan, M. J. *Nature* **1988**, *332*, 455. Watanabe, H.; Takehana, K.; Date, M.; Shinozaki, T.; Raz, A. *Cancer Res.* **1996**, *56*, 2960. Xu, W.; Seiter, K.; Feldman, E.; Ahmed, T.; W., C. J. *Blood* **1996**, *87*, 4502.
(8) Seeholzer, S. H. *Proc. Natl. Acad. Sci. U.S.A.* **1993**, *90*, 1237.
(9) Hansen, T.; Oehlmann, M.; Schönheit, P. *J. Bacteriol.* **2001**, *183*, 3428. Hansen, T.; Schlichting, B.; Grötzinger, J.; Swan, M. K.; Davies, C.; Schönheit, P. *FEBS J.* **2005**, *272*, 6266.

10.1021/ja710633c CCC: $40.75

Scheme 1. Fischer Projections of the Substrate, Inhibitor, and Analogue

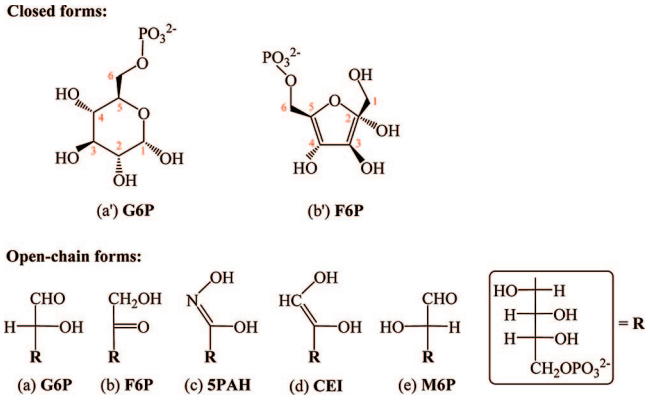

that the enzyme is a dimer with two α/β-sandwich domains in each subunit and the active sites are located between the two α/β domains at the interface between subunits.[15] The location of inhibitors leads to the identification of residues that may play roles in the catalysis, and as a consequence, several mechanisms have been proposed on the basis of general acid−base catalysis. Conventional PGIs, which are found in all domains of life, function without a metal cofactor, and the overall multistep catalytic mechanism consists of the ring-opening, isomerization, and ring-closing steps. Read et al. proposed a metal-independent isomerization mechanism in human PGI, where the conserved Glu357 and Lys518 in the active site play the general acid−base roles.[15] On the basis of rabbit and mouse PGI structures, however, Jeffery et al. and Graham Solomons et al. proposed that His388, which is also highly conserved, and Lys518 are involved in the catalytic mechanism and responsible for the formation of the *cis*-enediol intermediate.[6,20]

Recently, a novel type of PGI from the hyperthermophilic euryarchaeota species *Pyrococcus furiosus* (*Pf*), *Thermococcus litoralis* (*Tl*), and *Archaeoglobus fulgidus* (*Af*) has been identified and characterized.[9,22,23] These PGIs share no sequence similarity with the conserved PGI superfamily of eubacteria and eucarya. Crystallographic analysis has shown that this novel type of PGI contains a cupin fold comprising two β sheets,[12,18] and consequently the architecture of the enzyme is completely different from the $\alpha\beta\alpha$ fold in the conventional PGIs.[13,17,21,23] Strikingly, the cupin-type PGIs (cPGIs) contain a metal-binding site, which is located in the core of the cupin fold and can be found in most cupin enzymes, and thus constitute the metal-dependent PGI family.[13] Although cPGIs fall into the category of metalloenzyme, the exact role of the metal ion is still to be clarified, as it may be involved in substrate binding and/or catalysis.[17,18,23] It was initially suggested that the bound metal may be implicated only in substrate recognition, as the replacement or even the removal of the metal ion does not strongly influence the catalytic activity of *Pf*PGI.[18] But further analyses showed that the activity of the enzyme is completely lost after EDTA treatment, which depletes metal, and regained by the addition of metal.[24] Jeong et al. also showed a loss of catalytic function in *Tl*PGI mutants with no metals.[23] Hansen et al.'s depletion and reactivation experiments with cPGIs similarly confirmed the involvement of divalent cations in the catalytic mechanism.[10]

In general, the controversy over the reaction mechanism in PGIs focuses on the isomerization step, as both the ring-opening and ring-closing steps can be easily realized by the addition and deletion of a proton from the ring oxygen by the enzyme. As an aldose−ketose isomerization, the reversible conversion of the open-chain forms of G6P and F6P catalyzed by *Pf*PGI stoichiometrically involves the transfers of a hydrogen atom between the O1 and O2 oxygen atoms of the substrate (F6P/G6P) and another hydrogen between the C1 and C2 carbon atoms. The hydrogen transfer between C1 and C2 can occur either through a direct hydride shift or via a proton transfer involving a *cis*-enediol intermediate (Scheme 2).[2,17,21,24] Both mechanisms have been broadly adopted to decipher the hydrogen transfer in the enzymatic aldose−ketose isomerization. In the direct hydride-shift mechanism, the hydrogen transfer proceeds as a hydride, and the hydrogen atom of the substrate cannot exchange with the solvent. In contrast, in the *cis*-enediol intermediate mechanism, the hydrogen atom is transferred as a proton via a catalytic base, and it may exchange with the solvent. For conventional metal-independent PGIs, it has been well established that enzymes operate via the *cis*-enediol intermediate mechanism.[4,15] In isomerases such as xylose isomerase containing a metal ion at the catalytic center, the mechanism appears to be a hydride shift.[25] Indeed, the crystal structures of *Pf*PGI in native form and in complex with two active-site ligands, 5-phosphoarabinonate (5PAA) and gluconate 6-phosphate (G6P), show that the metal ion is not only adjacent to the C1−C2 region of the ligands but also coordinated by a glutamate residue (Glu97), which is thus unlikely to mediate the proton transfer in a *cis*-enediol mechanism.[17] Besides, the hydrophobic nature

(10) Hansen, T.; Schlichting, B.; Felgendreher, M.; Schönheit, P. *J. Bacteriol.* **2005**, *187*, 1621.
(11) Meng, M.; Chen, Y. T.; Hsiao, Y. Y.; Itoh, Y.; Bagdasarian, M. *Eur. J. Biochem.* **1998**, *257*, 500.
(12) Sun, Y. J.; Chou, C. C.; Chen, W. S.; Wu, R. T.; Meng, M. S.; Hsiao, C. D. *Proc. Natl. Acad. Sci. U.S.A.* **1999**, *96*, 5412.
(13) Dunwell, J. M.; Khuri, S.; Gane, P. *J. Microbiol. Mol. Biol. Rev.* **2000**, *64*, 153.
(14) Lee, J. H.; Chang, K. Z.; Patel, V.; Jeffery, C. J. *Biochemistry* **2001**, *40*, 7799.
(15) Read, J.; Pearce, J.; Li, X. C.; Muirhead, H.; Chirgwin, J.; Davies, C. *J. Mol. Biol.* **2001**, *309*, 447.
(16) Jeffery, C. J.; Hardre, R.; Salmon, L. *Biochemistry* **2001**, *40*, 1560. Arsenieva, D.; Hardre, R.; Salmon, L.; Jeffery, C. J. *Proc. Natl. Acad. Sci. U.S.A.* **2002**, *99*, 5872. Arsenieva, D.; Jeffery, C. J. *J. Mol. Biol.* **2002**, *323*, 77. Swan, M. K.; Hansen, T.; Schonheit, P.; Davies, C. *Proteins Pept. Lett.* **2003**, *10*, 517. Davies, C.; Muirhead, H.; Chirgwin, J. *Acta Crystallogr. D* **2003**, *59*, 1111. Richards, G. P. *Biochem Biophys. Acta* **2004**, *1702*, 89. Swan, M. K.; Hansen, T.; Schonheit, P.; Davies, C. *J. Biol. Chem.* **2004**, *279*, 39838. Lee, J.; Jeffery, C. J. *Protein Sci.* **2004**, *14*, 727. Milewski, S.; Janiak, A.; Wojciechowski, M. *Arch. Biochem. Biophys.* **2006**, *450*, 39.
(17) Swan, M. K.; Graham Solomons, J. T.; Beeson, C. C.; Hansen, T.; Schönheit, P.; Davies, C. *J. Biol. Chem.* **2003**, *278*, 47261.
(18) Berrisford, J. M.; Akerboom, J.; Turnbull, A. P.; de Geus, D.; Sedelnikova, S. E.; Staton, I.; McLeod, C. W.; Verhees, C. H.; van der Oost, J.; Rice, D. W.; Baker, P. J. *J. Biol. Chem.* **2003**, *278*, 33290.
(19) Swan, M. K.; Hansen, T.; Schonheit, P.; Davies, C. *Biochemistry* **2004**, *43*, 14088.
(20) Graham Solomons, J. T.; Zimmerly, E. M.; Burns, S.; Krishnamurthy, N.; Swan, M. K.; Krings, S.; Muirhead, H.; Chirgwin, J.; Davies, C. *J. Mol. Biol.* **2004**, *342*, 847.
(21) Berrisford, J. M.; Hounslow, A. M.; Akerboom, J.; Hagen, W. R.; Brouns, S. J. J.; van der Oost, J.; Murray, I. A.; Blackburn, G. M.; Waltho, J. P.; Rice, D. W.; Baker, P. J. *J. Mol. Biol.* **2006**, *358*, 1353.
(22) Verhees, C. H.; Huynen, M. A.; Ward, D. E.; Schiltz, E.; de Vos, W. M.; van der Oost, J. *J. Biol. Chem.* **2001**, *276*, 40926.
(23) Jeong, J. J.; Fushinobu, S.; Ito, S.; Jeon, B. S.; Shoun, H.; Wakagi, T. *FEBS Lett.* **2003**, *535*, 200.
(24) Berrisford, J. M.; Akerboom, J.; Brouns, S.; Sedelnikova, S. E.; Turnbull, A. P.; van der Oost, J.; Salmon, L.; Hardre, R.; Murray, I. A.; Blackburn, G. M.; Rice, D. W.; Baker, P. J. *J. Mol. Biol.* **2004**, *343*, 649.
(25) Whitlow, M.; Howard, A. J.; Finzel, B. C.; Poulos, T. L.; Winbourne, E.; Gilliland, G. L. *Proteins* **1991**, *9*, 153.

Scheme 2. Two Schemes of Reversible Isomerization Proposed in Previous Experimental Studies: (A) Hydride-Transfer Mechanism and (B) *cis*-Enediol Intermediate Mechanism

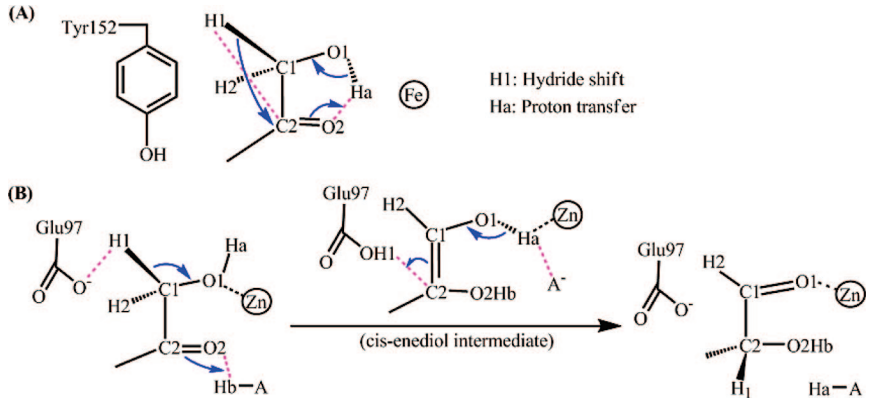

in the C1−C2 region also favors a hydride shift rather than a proton transfer between C1 and C2. Structural analyses further indicate that *Pf*PGI favors sugars in straight-chain forms rather than ring forms. Most recently, Berrisford et al. conducted NMR experiments which demonstrated that there is hydrogen exchange between the solvent and the substrate during the isomerization reaction catalyzed by *Pf*PGI, in accord with the *cis*-enediol intermediate mechanism.[21]

Although crystallographic studies have been able to present detailed yet static three-dimensional spatial arrangement of atoms of *Pf*PGI in native form and in complex with either substrates or inhibitors,[14,17,19,21,24,26] information about the dynamical conformational changes and particularly the transient conformations and the possible *cis*-enediol intermediate in the process of reactions is still out of reach. We note that the structural environment of the active domain in the reactive form may significantly differ from the static crystal configuration, as observed in the xylose isomerase[27] and the acyl-CoA dehydrogenase.[28] In fact, accumulating evidence shows that dynamics plays a critical role in the functions of proteins.[29] Computational studies have the potential to correlate the structures, dynamics, and functions of proteins and thus can complement experimental information,[30] and molecular dynamics (MD) simulations of enzymes at the atomic level can reveal the dynamic behavior of proteins in biological processes and provide insights into the physical mechanisms and the physical principles underlying these processes.[31]

To probe the dynamics and functions of proteins and reconcile the proposed distinct mechanisms for metal-dependent PGIs, we have performed combined quantum mechanics (QM)/molecular mechanics (MM) calculations and MD simulations on the aldose−ketose isomerization reaction catalyzed by *Pf*PGI. A possible mechanism for the reversible isomerization, the stereochemistry selectivity in the hydride transfer, and the roles of the conserved residues and the metal ion have been investigated and elucidated.

Computational Details

Computational Models. Since the goal of our present QM/MM study is to elucidate the catalytic mechanism and identify the transition state in the aldose−ketose isomerization, computations began with the Michaelis complex of the enzymatic reaction. However, experimentally, the structure of a Michaelis complex is in general difficult to detect,[32] as the complex would instantly lead to the product state under the regular experimental conditions. Computationally, Michaelis complex models were generated on the basis of the crystal structure of *Pf*PGI in complex with 5-phospho-D-arabinonohydroxamate (5PAH, see Scheme 1) and zinc at the resolution of 2.0 Å (PDB code 2GC0),[21] and the *Pf*PGI-5PAH structure is very similar to the *Pf*PGI-F6P crystal structure (PDB code 2GC2; see Figure 1Sa,b in Supporting Information). After the inhibitor 5PAH was substituted by the *cis*-enediol intermediate or the substrate F6P, the complete enzyme−substrate model was solvated into a water sphere of 30 Å radius centered on the Zn^{2+} ion. Water molecules less than 2.5 Å from the enzyme were removed from the system. The hydrogen atoms of the protein and the crystal water were incorporated using the HBUILD facility in CHARMM[33] on the basis of heavy-atom positions and standard bond lengths and angles. CHARMM22 and CHARMM27 force fields were employed to represent all of the MM atoms during the setup of models.[34] In consideration of the experimental condition, the histidine residues were assigned to the neutral HSD in both complex models. The protonated Glu97 residue in the complex of *Pf*PGI with F6P was considered in MD simulations, since the (F6P)—O2···O—(Glu97) distance in the crystal structure (PDB code 2GC2) of the complex is about 2.85 Å and thus suggests an ideal hydrogen bond.[21] The partial charge parameters of substrates were based on the Mulliken population analysis from the QM(B3LYP) calculations. The final model of the complex with F6P consisted of 12 198 atoms, including the *Pf*PGI protein, 3058 water molecules, and 10 sodium ions to neutralize the whole system. To get adequate models for the subsequent computations, initial

(26) Cordeiro, A. T.; Michels, P. A. M.; Delboni, L. F.; Thiemann, O. H. *Eur. J. Biochem.* **2004**, *271*, 2765.
(27) Lavie, A.; Allen, K. N.; Petsko, G. A.; Ringe, D. *Biochemistry* **1994**, *33*, 5469. Garcia-Viloca, M.; Alhambra, C.; Truhlar, D. G.; Gao, J. L. *J. Comput. Chem.* **2003**, *24*, 177. Garcia-Viloca, M.; Poulsen, T. D.; Truhlar, D. G.; Gao, J. L. *Protein Sci.* **2004**, *13*, 2341.
(28) Poulsen, T. D.; Garcia-Viloca, M.; Gao, J. L.; Truhlar, D. G. *J. Phys. Chem. B* **2003**, *107*, 9567. Satoh, A.; Nakajima, Y.; Miyahara, I.; Hirotsu, K.; Tanaka, T.; Nishina, Y.; Shiga, K.; Tamaoki, H.; Setoyama, C.; Miura, R. *J. Biochem.* **2003**, *134*, 297. Bhattacharyya, S.; Stankovich, S.; Truhlar, D. G.; Gao, J. L. *Biochemistry* **2005**, *44*, 16549.
(29) Eisenmesser, E. Z.; Bosco, D. A.; Akke, M.; Kern, D. *Science* **2002**, *295*, 1520. Eisenmesser, E. Z.; Millet, O.; Labeikovsky, W.; Korzhnev, D. M.; Wolf-Watz, M.; Bosco, D. A.; Skalicky, J. J.; Kay, L. E.; Kern, D. *Nature* **2005**, *438*, 117.
(30) Benkovic, S. J.; Hammes-Schiffer, S. *Science* **2003**, *301*, 1196. Garcia-Viloca, M.; Gao, J.; Karplus, M.; Truhlar, D. G. *Science* **2004**, *303*, 186. Agarwal, P. K. *J. Am. Chem. Soc.* **2005**, *127*, 15248.
(31) Warshel, A. *Annu. Rev. Biophys. Biomol. Struct.* **2003**, *32*, 425. Karplus, M.; Kuriyan, J. *Proc. Natl. Acad. Sci. U.S.A.* **2005**, *102*, 6679. Hammes-Schiffer, S. *Acc. Chem. Res.* **2006**, *39*, 93. König, P. H.; Ghosh, N.; Hoffmann, M.; Elstner, M.; Tajkhorshid, E.; Frauenheim, T.; Cui, Q. *J. Phys. Chem. A* **2006**, *110*, 548. Lin, Y.; Cao, Z.; Mo, Y. *J. Am. Chem. Soc.* **2006**, *128*, 10876.
(32) Lahiri, S. D.; Zhang, G.; Dunaway-Mariano, D.; Allen, K. N. *Science* **2003**, *299*, 2067.
(33) Brooks, B. R.; Bruccoleri, R. E.; Olafson, B. D.; States, D. J.; Swaminathan, S.; Karplus, M. *J. Comput. Chem.* **1983**, *4*, 187.
(34) MacKerell, A. D., Jr.; et al. *J. Phys. Chem. B* **1998**, *102*, 3586.

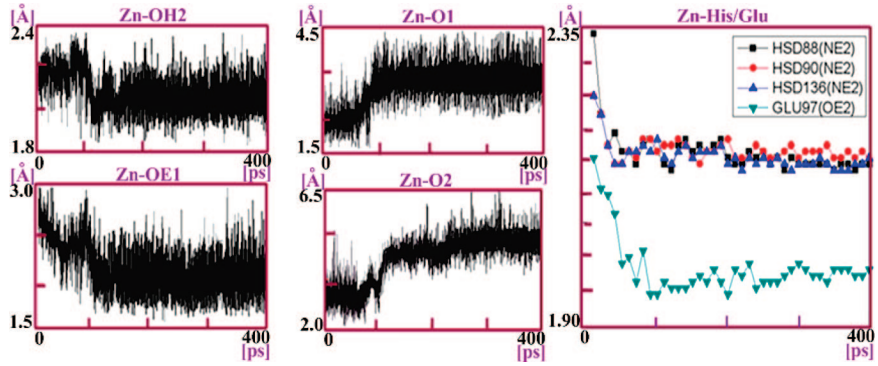

Figure 1. Time evolution of several internuclear distances in the 400 ps MM MD simulation. The selected distances are associated with the coordination shell of Zn^{2+}, where OH2 is the oxygen atom of crystal water 97, OE1 denotes the carboxylate oxygen of Glu97, and O1 and O2 are from the substrate F6P.

MD simulations at the MM level were performed for 400 ps. In the simulations, the temperature was maintained at 300 K, and all of the bonds with hydrogen atoms in the MM part were constrained with the SHAKE algorithm.[35]

QM(B3LYP)/MM Calculations. The QM/MM calculations concern a QM region with 52 QM atoms in the reactive site (including residues Glu97, His158, and Glu61, a chain of five water molecules, the Zn^{2+} ion, the truncated substrate, and four hydrogen link atoms) and 12 150 MM atoms. In the QM/MM geometry optimizations, the QM region and 2014 MM atoms (defined by including all residues within 15 Å of Zn^{2+}) were allowed to relax, whereas the remaining MM atoms were frozen. The QM part was treated at the B3LYP/6-31G(d) level, and the MM part was described by the CHARMM22 and CHARMM27 force fields. An electronic embedding scheme[36] incorporating the MM charges into the one-electron Hamiltonian of the QM treatment and hydrogen link atoms with charge shift model[37] for the QM/MM boundary were adopted in the QM/MM treatment. The ChemShell package[38] integrating the Turbomole[39] and DL-POLY[40] programs was employed to perform the QM/MM computations. The default convergence criteria were adopted in the QM/MM geometry optimization with the HDLC optimizer[41] for complexes of the enzyme with the substrates F6P and G6P, as well the intermediates involved in reactions. For comparison, QM/MM optimization with a larger QM region including the whole substrate F6P was performed for the equilibrated configuration of the *Pf*PGI-F6P complex from 400 ps MM MD simulations. Both QM/MM calculations with different QM regions predict quite similar active domains. In comparison with the QM/MM calculation with the truncated substrate, the phosphate moiety of the substrate was almost unchanged in the full optimization of the substrate due to strong hydrogen-bond network around it. An elaborated configuration from the potential energy surface scan served as the initial structure in the transition-state search.

QM(PM3)/MM MD Simulations. The stationary points obtained from the above QM(B3LYP)/MM optimizations were taken as the initial structures for the QM/MM MD simulations. All QM/MM MD simulations were performed at the PM3[42]/CHARMM level with the ChemShell package, which provides the QM/MM coupling engine and the MD driver. The energy and gradient evaluations for the QM and MM parts were conducted by using the MNDO99[43] and DL-POLY codes, respectively. The QM region (where four water molecules near the outer shell of the active domain were frozen) and the active MM atoms defined in the QM/MM calculations were used in the subsequent QM/MM MD simulations. The QM/MM MD setup and thermodynamic integration approach have been introduced in previous works.[44] The MD simulations were performed at temperature of 300 K under the NVT canonical ensemble. The system was first heated by using a Berendsen thermostat[45] for 10 ps and then equilibrated by using a Nosé-Hoover thermostat[46] for another 10 ps. Afterward, the system was sampled every 5 ps along the reaction coordinate, and the restart files for all windows on the reaction coordinate were prepared. Finally, each point on the reaction coordinate was propagated for 5 ps to generate the data for thermodynamic integrations. Statistical tests, such as the Mann−Kendall[47] test for trend, the Shapiro−Wilk W[48] test for normality, and the von Neumann[49] test for serial correlation, were performed to establish converged averages.

Results and Discussion

A. Initial Conformation of the Active Site. The reported crystal structures of *Pf*PGIs indicate that the coordination shell of the central metal ion Zn^{2+} is flexible to some extent in various complexes.[14,17,19,21,24,26] It is thus a prerequisite to determine the coordination structure of Zn^{2+} during catalysis in order to rationally propose a consistent catalytic mechanism. Our MD simulations and QM(B3LYP)/MM calculations showed that the coordination shell of Zn^{2+} changes significantly from the initial static crystal conformation to the equilibrated state of the enzyme-F6P complex which is now solvated in aqueous solution. Figure 1 plots selected time-dependent interatomic distances, and the equilibrium conformations from the 400 ps MM MD simulation are shown in Figure 2a,b.

As Figure 1 shows, the profile of the MD trajectories clearly exhibits that a crystal water molecule, CW97 (HOH97 in 2GC0), gradually enters the coordination shell of the Zn^{2+} ion during

(35) van Gunsteren, W. F.; Berendsen, H. J. C. *Mol. Phys.* **1977**, *34*, 1311.
(36) Bakowies, D.; Thiel, W. *J. Phys. Chem.* **1996**, *100*, 10580.
(37) de Vries, A. H.; Sherwood, P.; Collins, S. J.; Rigby, A. M.; Rigutto, M.; Kramer, G. J. *J. Phys. Chem. B* **1999**, *103*, 6133. Sherwood, P.; de Vries, A. H.; Collins, S. J.; Greatbanks, S. P.; Burton, N. A.; Vincent, M. A.; Hillier, I. H. *Faraday Discuss.* **1997**, *106*, 79.
(38) Sherwood, P.; et al. *Theochem—J. Mol. Struct.* **2003**, *632*, 1.
(39) Ahlrichs, R.; Bar, M.; Haser, M.; Horn, H.; Kolmel, C. *Chem. Phys. Lett.* **1989**, *162*, 165.
(40) Smith, W.; Forester, T. R. *J. Mol. Graph.* **1996**, *14*, 136.
(41) Billeter, S. R.; Turner, A. J.; Thiel, W. *PCCP* **2000**, *2*, 2177.
(42) Stewart, J. J. P. *J. Comput. Chem.* **1989**, *10*, 209. Stewart, J. J. P. *J. Comput. Chem.* **1989**, *10*, 221.
(43) Thiel, W. *MNDO99*,version 6.1; Max-Planck-Institut für Kohlenforschung: Mülheim an der Ruhr, Germany, 2003.
(44) Beveridge, D. L.; Dicapua, F. M. *Annu. Rev. Biophys. Biophys. Chem.* **1989**, *18*, 431. Straatsma, T. P.; McCammon, J. A. *J. Chem. Phys.* **1991**, *95*, 1175. Senn, H. M.; Thiel, S.; Thiel, W. *J. Chem. Theory Comput.* **2005**, *1*, 494.
(45) Berendsen, H. J. C.; Postma, J. P. M.; van Gunsteren, W. F.; DiNola, A.; Haak, J. R. *J. Chem. Phys.* **1984**, *81*, 3684.
(46) Nosé, S. *J. Chem. Phys.* **1984**, *81*, 511. Nosé, S. *Mol. Phys.* **1984**, *52*, 255.
(47) Schiferl, S. K.; Wallace, D. C. *J. Chem. Phys.* **1985**, *83*, 5203.
(48) Shapiro, S. S.; Wilk, M. B. *Biometrika* **1965**, *52*, 591.
(49) von Neumann, J. *Ann. Math. Stat.* **1941**, *12*, 367.

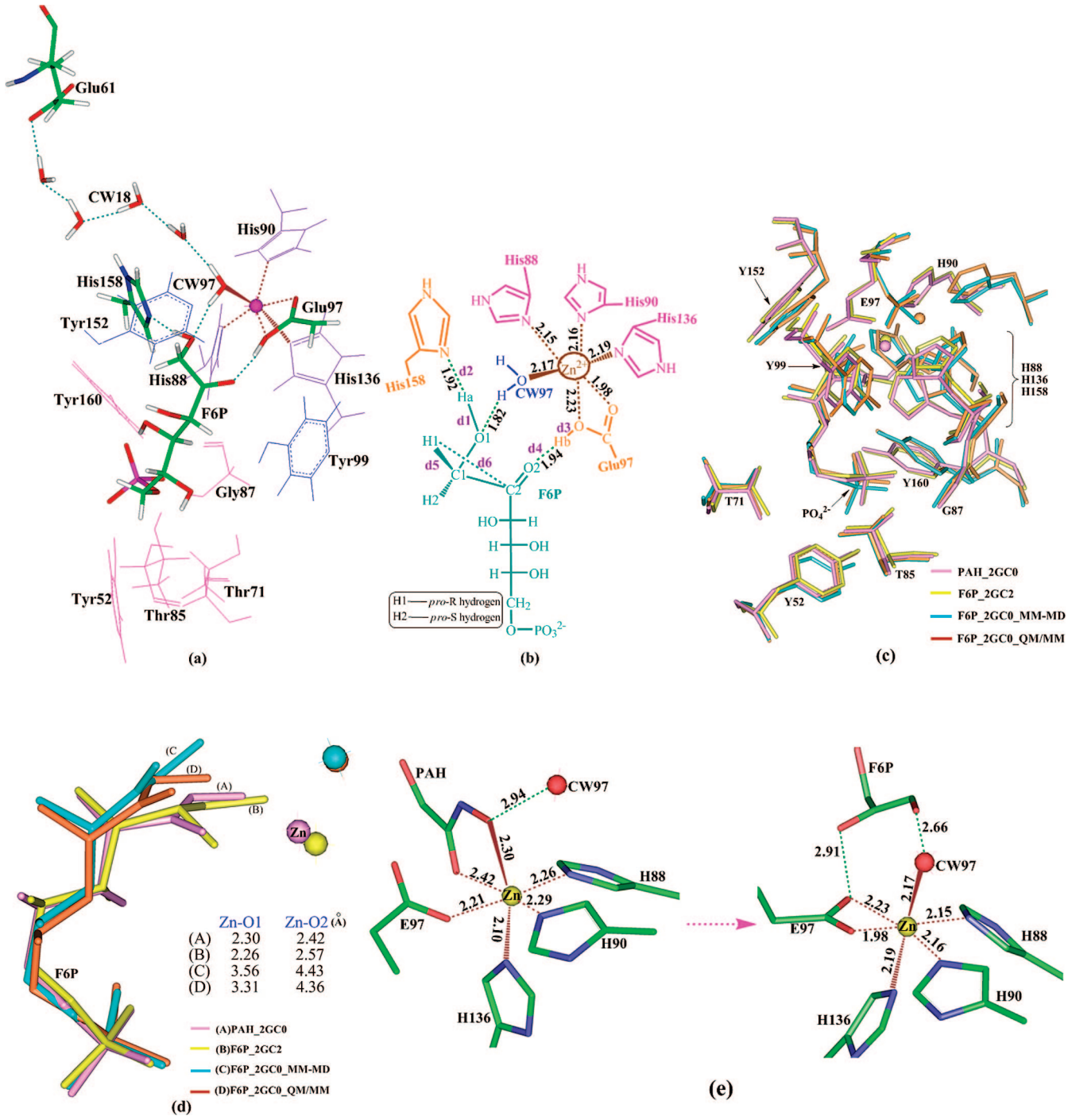

Figure 2. (a,b) Equilibrium conformations of the *Pf*PGI in complex with F6P. (c,d) Superimposition of four structures, 2GC0, 2GC2, the equilibrated 2GC0 by MM MD simulation for 400 ps, and the QM/MM-optimized 2GC0 based on the equilibrated 2GC0. (e) Coordination-shell change of Zn^{2+} and relaxation of the surrounding hydrogen-bond network from the static crystal structure to the equilibrated configuration in solution.

MD simulations within the first 100 ps, whereas the carboxylate group of Glu97 tends to bind to the metal ion closely, along with the conversion from a monodentate to a bidentate coordination. In contrast, F6P loses the direct contact with Zn^{2+} after about 100 ps. The coordination of three histidine residues to Zn^{2+} changes little during the MD simulations. As a consequence, in the equilibrated state, the Zn^{2+} ion is hexacoordinated by the carboxylate group (both OE1 and OE2 atoms) of Glu97, a water molecule, and the nitrogen (NE2) atoms in the pyridine groups of His88, His90, and His136, while the binding of the O1/O2 atoms of F6P to Zn^{2+} observed in the crystal structure no longer survives. (A detailed comparison of the coordination shell is shown in Figure 1S in Supporting Information.) As Figure 2c,d displays, such changes of the coordination shell of Zn^{2+} basically arise from the relaxation of the surrounding hydrogen-bond network, along with the repositioning of the residue Glu97, the substrate F6P, and Zn^{2+}, as shown in Figure 2e. The depletion of solvent molecules might result in crystal structures different, to some extent, from the true conformations in enzymatic catalysis which occur in the solvent environment.[27] Our MD simulations also revealed an ideal hydrogen bond wire between Zn^{2+} and the carboxylate

Scheme 3. Possible Zwitterionic Intermediate-Based Mechanism Proposed in This Work for the Reversible Isomerization of F6P and G6P, Where Glu97 and His158 Play the Roles of General Acid/Base

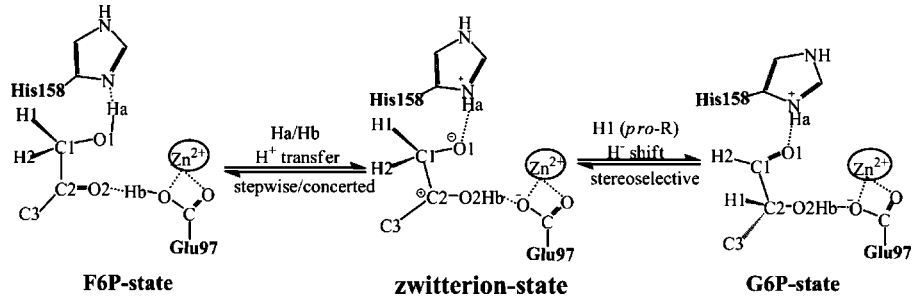

group CO_2^- of Glu61 through five water molecules (see Figure 2a). The C1−C2 moiety of the substrate F6P is bound in the active site through hydrogen-bond interactions between F6P and the residues Glu97 and His158, as well the Zn^{2+}-bound water (see Figure 2b). Most of conserved residues are found in the vicinity of F6P. In particular, the hydrophobic residues Tyr152 and Tyr99 are located on both sides of the C1−C2 region, constructing a local hydrophobic environment toward the H1C1−C2 side of substrate. Other conserved residues (Tyr52, Tyr160, Thr71, Thr85, and Gly87), located at the bottom of the active pocket,[17,18,21] constitute a complicated hydrogen-bond network with the hydroxyl and phosphate groups of F6P, which essentially retains their initial configurations in the process of reaction (*vide infra*; see Figures 2S and 3S in Supporting Information).

B. The Enzymatic Reaction. On the basis of our QM/MM calculations and MD simulations, a zwitterion intermediate mechanism was put forward as illustrated in Scheme 3. Before further computational verifications for this mechanism, we note that the dual-specificity type of phosphoglucose/phosphomannose isomerase (PGI/PMI), from *Pyrobaculum aerophilum* can catalyze the conversions of both F6P/G6P and F6P/M6P (open-chain form of mannose 6-phosphate, see Scheme 1) at equal rates.[19] It was assumed that the *cis*-enediol mechanism is responsible for the PMI reaction and its PMI activity arises from the additional space imparted by a threonine residue (Thr291). The PGI/PMI enzyme has structure similar to that of *Pf*PGI, and the replacement of the substrate G6P by M6P in the equilibrated configuration results in a complex in which the O2 of M6P is in the opposite direction as compared with the O2 of G6P. As a result, there is no base like the residue Glu97 in the vicinity of M6P to drive the proton transfer. Presumably, the internal rotation of M6P around the C2−C3 bond, prior to the proton transfer catalyzed by *Pf*PGI, is necessary. However, such rotation is unlikely to occur for *Pf*PGI due to the severe spatial and energetic (hydrogen bond) constraints around M6P. Thus, *Pf*PGI is unable to isomerize M6P; in other words, it is highly specific for its substrates, just like other conventional PGIs. In contrast, rotation around the C2−C3 bond was proved to be facile for PGI/PMI enzymes, where the presence of a threonine residue (Thr291) in the place of a glutamine in conventional PGIs creates a relatively large space for the active site.[19]

QM(B3LYP)/MM Optimizations. The B3LYP QM/MM calculations were performed to evaluate the relative energies of the F6P reactant, intermediates, transition states, and the G6P product in the enzymatic environment. Figure 3 presents the relative energy profiles along possible isomerization routes.

As demonstrated by Figure 2, there is strong substrate−enzyme interaction in the F6P-PGI complex due to the existence of stabilizing hydrogen bonds between the substrate F6P and the residues His158 and Glu97. The corresponding hydrogen-bond network may mediate the hydrogen transfers between the substrate and the surrounding residues, where His158 can serve as a catalytic base to abstract the proton (Ha) from O1 of F6P, and Glu97 behaves as a proton donor (Hb) to O2 of F6P. These hydrogen (Ha/Hb) transfers may proceed through a stepwise or concerted mechanism. In the stepwise process (**F6P→ts1→im→ts2→zwitterion**, see Figure 3), the deprotonation (Ha) from F6P leads to an intermediate (**im**) with a barrier of only 3.6 kcal/mol. The intermediate subsequently accepts a proton (Hb) from Glu97 to yield a slightly more stable intermediate (**zwitterion**), and this process experiences a negligible barrier of 0.3 kcal/mol and can occur instantly. The hydrogen (Ha/Hb) transfers can be characterized by the moiety changes: [O1Ha]→$[O1]^-$/[C2O2]→$[C2O2Hb]^+$. Thus, the resultant intermediate can be viewed as a zwitterionic intermediate, as suggested by the charge populations listed in Table 1. In the concerted process (**F6P→TS1→zwitterion**), both the Ha and Hb transfers occur simultaneously, and the activation energy for the formation of the zwitterionic intermediate is 3.5 kcal/mol. On the basis of the present QM(B3LYP)/MM calculations, we thus conclude that the concerted and stepwise processes are comparable energetically and can both proceed effectively.

At the stage of the zwitterionic intermediate, there are two possibilities for the hydrogen transfer between C1 and C2: the *pro*-R H1 shift, which generates the *pro*-R G6P, or the *pro*-S H2 shift, which yields the *pro*-S G6P. The QM(B3LYP)/MM calculations predict that the barriers for the isomerization of the zwitterionic intermediate to the *pro*-R and *pro*-S G6P are 5.4 and 7.0 kcal/mol, respectively. Notably, the *pro*-R H1 transfer from C1 to C2 is more favorable than the *pro*-S H2 dynamically, and this advantage of H1 over H2 can be linked to the specific stereochemistry of the protein environment around the substrate (*vide infra*).

During the hydrogen-transfer process from C1 to C2 (**zwitterion→G6P**), the Mulliken positive charges at C1 increase from −0.09 to 0.24 e, whereas the positive charges at C2 remarkably decrease from 0.43 to 0.03 e, as shown in Table 1, suggesting that the hydrogen transfer from C1 to C2 is a hydride-shift process. The relative energies shown in Figure 3 indicate that the overall isomerization reaction from F6P to G6P need overcome a barrier of less than 8 kcal/mol. If we consider that the zero-point energy and proton tunneling generally reduce the barrier height by 2−3 kcal/mol, the reversible interconversion between F6P and G6P is extremely facile.

To probe the possibility of a direct hydrogen transfer from O1 to O2 involved in the isomerization process, as suggested in the hydride-transfer mechanism (Scheme 2), we conducted relevant QM(B3LYP)/MM optimizations to locate the transition states and estimate the reaction barriers. Predicted barriers for

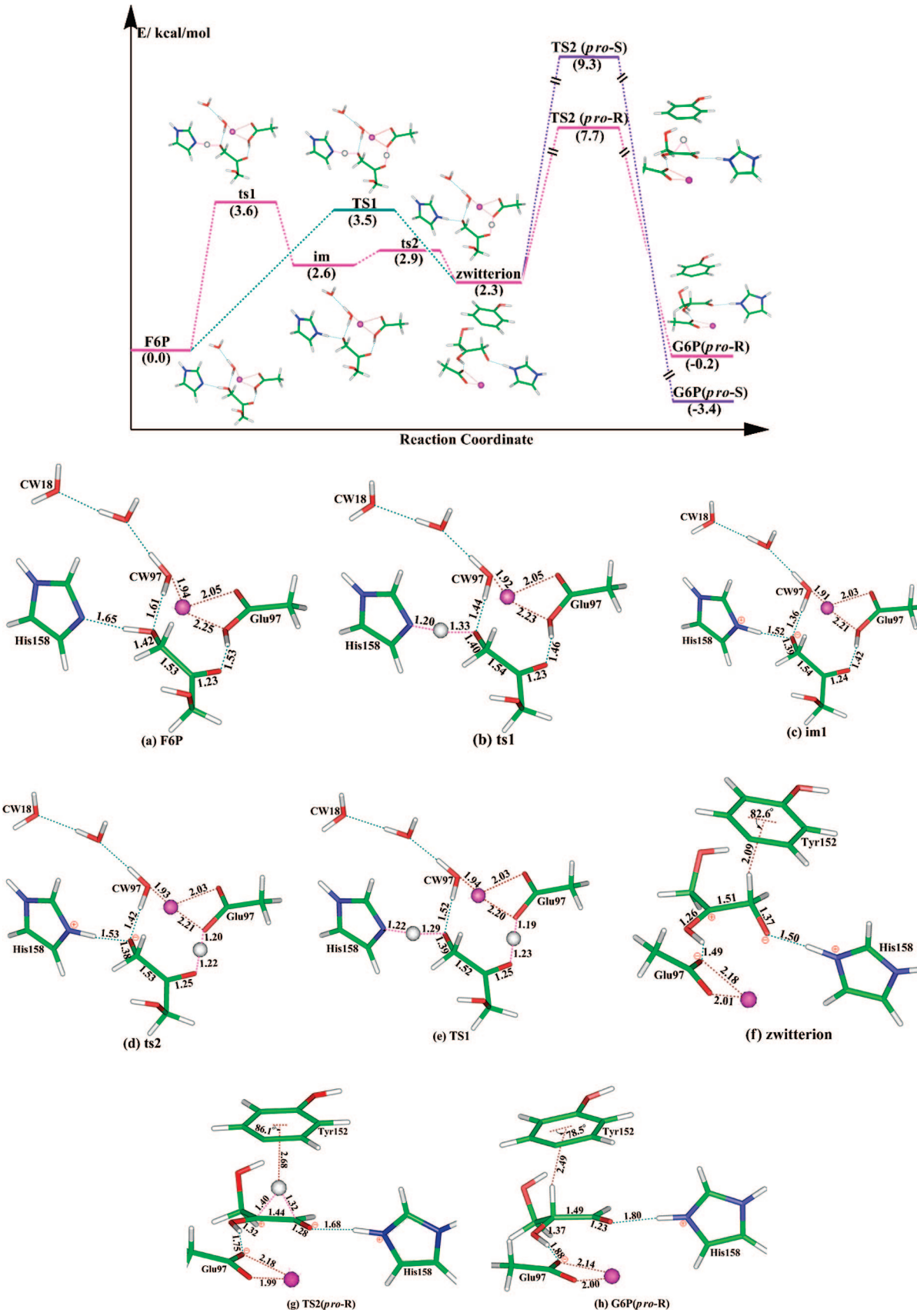

Figure 3. QM/MM relative energy profiles along the zwitterionic intermediate path and the QM/MM-optimized conformations of complexes involved in isomerization (the bond lengths are given in angstroms and bond angles in degrees). Only a few residues in the active site are shown for simplicity (in structures **f**, **g**, and **h**, residue Tyr152 is shown in order to give insight into its role in facilitating the hydride transfer).

the rate-determining step in the stepwise and concerted mechanisms are about 27 and 24 kcal/mol, respectively. Accordingly, our calculations exclude the possibility of direct hydrogen transfer from O1 to O2 in the enzymatic catalysis.

Table 1. Mulliken Charge Populations of Selected Atoms in the Active Sites of *Pf*PGI at Their Different Reactive States

	substrate								
state	Ha	Hb	H1	O1	O2	C1	C2	OE1 (Glu97)	NE2 (His158)
F6P	0.48	0.49	0.21	−0.71	−0.45	−0.13	0.44	−0.63	−0.55
ts1	0.47	0.50	0.19	−0.73	−0.46	−0.10	0.44	−0.55	−0.60
im	0.44	0.50	0.18	−0.72	−0.46	−0.09	0.43	−0.64	−0.59
ts2	0.44	0.52	0.19	−0.71	−0.47	−0.08	0.44	−0.65	−0.59
TS1	0.47	0.52	0.20	−0.72	−0.47	−0.10	0.45	−0.65	−0.60
zwitterion	0.44	0.51	0.20	−0.70	−0.45	−0.09	0.43	−0.63	−0.59
TS2	0.44	0.47	0.25	−0.59	−0.56	−0.04	0.25	−0.60	−0.59
G6P	0.41	0.45	0.21	−0.44	−0.70	0.24	0.03	−0.58	−0.57

Table 2. Predicted Imaginary Frequencies for the Transition States and KIE Values for Corresponding Hydrogen-Transfer Processes

	frequencies (cm^{-1})		H/D KIE	
TS	H	D	KIE^{semi}	KIE^{Wigner}
ts1	−281.9	−237.6	3.22	3.3
ts2	−453.5	−339.9	2.91	3.1
TS1	−818.4	−594.2	8.01	9.6
TS2	−796.5	−779.0	1.53	1.6

Kinetic Isotope Effect. To approximately evaluate the nuclear quantum dynamical effect on the proton transfer in *Pf*PGI, we calculated the semiclassical kinetic isotope effect (KIE) based on the QM region (52 atoms) defined in the QM/MM calculation. The required free energy of activation and vibrational frequencies were determined at the B3LYP/6-31G* level by using the Gaussian03 package.[50] Both the semiclassical KIE values and the Wigner-corrected[51] KIE values for the proton/hydride-transfer processes are compiled in Table 2. Interestingly, our results show that the concerted proton-transfer process exhibits much larger KIE and Wigner tunneling correction with respect to the stepwise process, implying that there is a pronounced quantum mechanical tunneling effect in the concerted process. However, the barriers for the proton/hydride transfers are so small (3.5−5.4 kcal/mol) that the tunneling effect is expected to be insignificant in the reversible isomerization process catalyzed by *Pf*PGI.

QM(PM3)/MM MD Simulations. The QM/MM MD simulations have been performed to derive the Helmholtz free-energy profiles for the isomerization process. The QM region was treated at the PM3 level to reduce the computational costs. The reaction coordinates (RC) were defined as follows (see Figure 2): RC1 = d1−d2 (in the range of −1.8 to 1.8 bohrs) for the first proton (Ha) transfer; RC2 = d3−d4 (in the range of −1.6 to 1.8 bohrs) for the second proton (Hb) transfer; and RC3 = d5−d6 (in the range of −2.2 to 2.4 bohrs) for the hydride (H1) transfer. An integration step of 0.2 bohr along the RCs was used. The resulting free-energy profiles for the isomerization reaction are depicted in Figure 4, and detailed thermodynamic integration data are compiled in Tables 1S−4S in Supporting Information. Notably, the free energies of activation for the proton/hydride transfers shown in Figure 4 are in reasonable agreement with the relative QM(B3LYP)/MM energetics in Figure 3, although the magnitudes of the reaction free energies obtained by QM(PM3)/MM MD simulations are somewhat higher than the B3LYP QM/MM values. Of significance, the QM(PM3)/MM MD simulations showed that the H1 is much more active than the H2 in the hydride-transfer step. The relatively high activity of the *pro*-R H1 of F6P has been observed in previous experiments.[21,52]

C. Roles of Conserved Residues and the Metal Ion. Tyr152 and Tyr99. It has been assumed in previous studies that Tyr152 provides the dominant force to promote the hydride shift.[17,18] A similar view was proposed by Xiao et al. in their computational study of human phosphomannose isomerase.[53] To appreciate the roles of residues Tyr152 and Tyr99 in the catalysis, we performed QM(B3LYP)/MM calculations on the mutated system with the replacement of both Tyr99 and Tyr152 by alanine. Results indicated that the barrier for the hydride (H1) transfer from C1 to C2 is 8.1 kcal/mol, 2.7 kcal/mol higher than the corresponding activation energy for the wild-type *Pf*PGI. We note that the residues Tyr152 and Tyr99 locate in the two sides of the substrate in the zwitterionic conformation (**zwitterion**), where the C1−H1 bond points to the aromatic ring of Tyr152 (see Figure 3), while the side chain of Tyr99, bound to the bottom of F6P/G6P through hydrogen-bond interactions with the involvement of one water molecule, is far away from the C1−C2 region. The aromatic ring of Tyr152 stacking over H1 may facilitate the hydride (H1) transfer due to the hydrophobic (van der Waals) repulsive interactions. In contrast, the anticipated cation−π interactions between the aromatic ring of Tyr152 and H^+ make the proton-shift process less favorable energetically. Furthermore, the presence of the positively charged carbon (C2) in **zwitterion** may promote the hydride transfer. Tyr99, together with other residues, confines the substrate in the active pocket (*vide infra*).

Other Conserved Residues. Besides Tyr99 and Tyr152, the rest of the highly conserved residues, including Tyr52, Thr71, Thr85, Gly87, and Tyr160, have been found to be important in the catalysis of *Pf*PGI. But the role of these residues as primarily either structural or functional has not been well understood.[18] Here we studied the homology structure of the Ala mutant by substituting the above conserved residues with alanines and compared the binding interactions of the substrate F6P with the native *Pf*PGI and its Ala variant computationally, based on the MD simulations for 400 ps. As shown in Figure 5, the equilibrated distances of Ha···NE2 (His158) and O2···Hb in the native enzyme are about 1.92 and 1.94 Å, respectively. However, both separations increase to about 2.70 and 2.40 Å in the Ala mutant. The increased distances indicate that the hydrogen atoms (Ha/Hb) are less accessible, and thus the hydrogen transfer is unlikely to occur in the Ala mutant. The present MD simulation results led to the conclusion that the primary role of these conserved residues is to maintain the substrate in the near-attack reactive conformation (NAC). The

(50) Frisch, M. J. *Gaussian 03*, revision C.02; Gaussian, Inc.: Wallingford, CT, 2004.
(51) Melander, L.; Sauders, W. H., Jr. *Reaction Rates of Isotopic Molecules*; Robert E. Krieger Publishing Co.: Malabar, FL, 1987.
(52) Rose, I. A.; O'Connell, E. L. *Biochim. Biophys. Acta* **1960**, *42*, 159.
(53) Xiao, J. F.; Guo, Z. R.; Guo, Y. S.; Chu, F. M.; Sun, P. Y. *J. Mol. Graph. Model.* **2006**, *25*, 289.

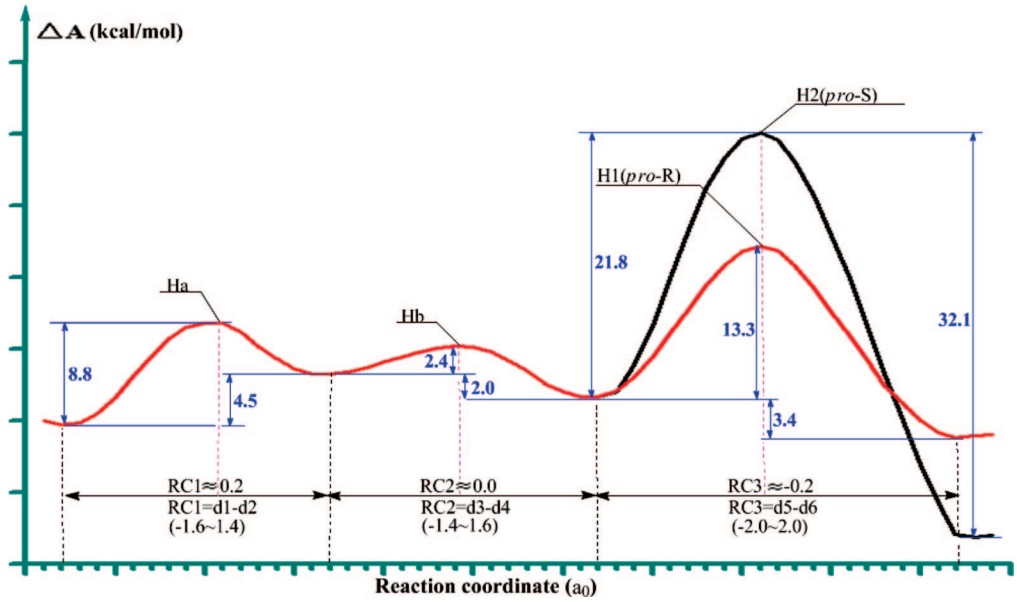

Figure 4. Free-energy difference profiles along the different reaction coordinates (refer to Figure 2b). The plot consists of three reaction steps, the reaction coordinates of which are assigned as RC1, RC2, and RC3, respectively.

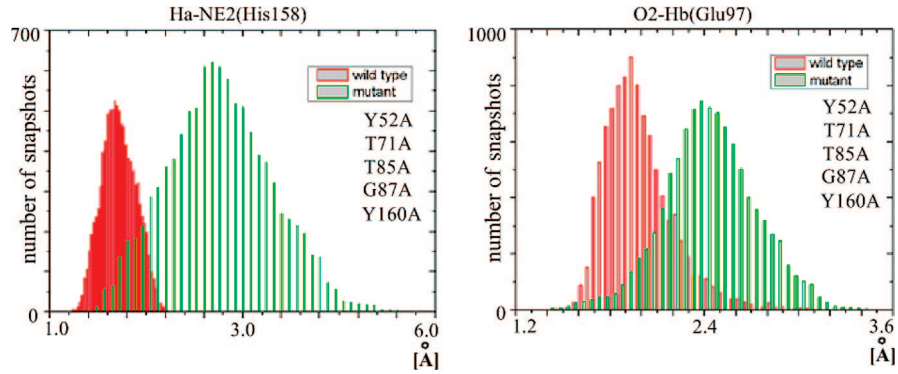

Figure 5. Fluctuations of the Ha−NE2 and O2−Hb distances in the 400 ps MD simulations of wild-type *Pf*PGI and its alanine mutant for the conserved residues in complex with F6P.

NAC effect on the enzymatic reaction has been extensively explored in chorismate mutase and haloalkane dehalogenase[54] and verified to play a crucial role in catalysis.

Zinc. The presence of a metal-binding site is a disparate hallmark of this fold in *Pf*PGI in comparison with the conventional PGI. The role of the metal ion in the enzymatic catalysis was well established by extensive experimental studies.[10,17,18,21,23] In Hansen et al.'s experiment,[10] treatment with EDTA disabled the catalytic activity of cPGIs completely, and addition of some divalent cations, such as $ZnCl_2$, can reactivate the enzyme. Similarly, the removal of metal ion in *Pf*PGI[18] and *Tl*PGI[23] leads to either little or dramatic loss of catalytic activity. As such, the Zn^{2+} ion may participate in the reaction directly and/or facilitate the reaction indirectly by binding the substrate. It should be pointed out that, in Jeong et al.'s experiment, the conserved histidine and glutamate residues were mutated in order to make the cupin motif unable to retain metal ions.[23] Our QM/MM calculations indicate that the coordination shell of Zn^{2+} is essentially unchanged in the catalytic process, and the metal ion acts as a structural anchor to maintain Glu97 at a proper position for mediating the proton transfer.

While Zn^{2+} is hexacoordinated in all conformations in our computations, it relates to the substrate through a water chain, where the hydrogen-bond interactions are enhanced by the electrostatic interaction from the positively charged metal ion. This hydrogen bond wire links Zn^{2+} and the substrate as well as the outer region as shown in Figure 2a, and it may serve as a channel for hydrogen exchange between substrate and solvent, as observed experimentally.[21] To explore the possibility of such a hydrogen-exchange channel, we performed primary calculations on a *cis*-enediol−ZnOH model, which derived from the proton transfer (*pro*-R H1) from C1 to O1, along with the proton transfer between the Zn-bound water to Glu61 through the water chain. The QM(B3LYP)/MM calculations predict that the transformation of the zwitterionic intermediate (**zwitterion**−$ZnOH_2$) to the *cis*-enediol−ZnOH conformation must overcome a barrier of 13.6 kcal/mol, with an endothermicity of 3.6 kcal/mol (see Figure 6). Once the *cis*-enediol intermediate is formed, the *pro*-R H1 linking to O1 may exchange with a hydrogen of the solvent through the water chain, as shown in Figure 6. Previous studies show that the

(54) Lau, E. Y.; Kahn, K.; Bash, P. A.; Bruice, T. C. *Proc. Natl. Acad. Sci. U.S.A.* **2000**, *97*, 9937–9942. Zhang, X.; Bruice, T. C. *Proc. Natl. Acad. Sci. U.S.A.* **2005**, *102*, 18356.

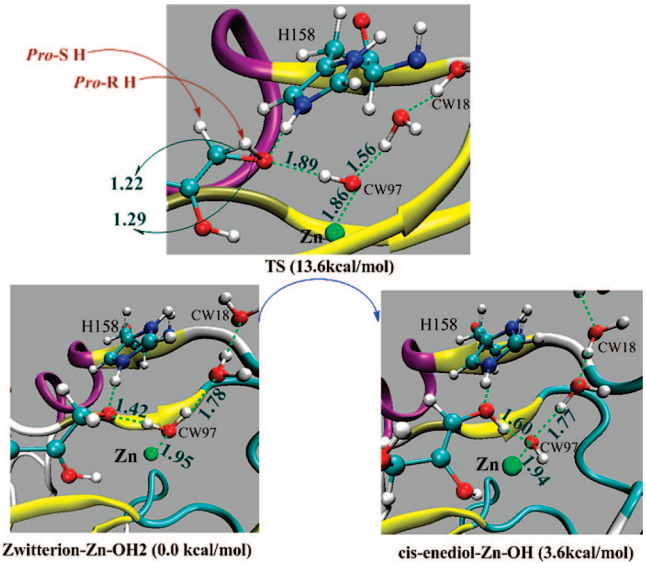

Figure 6. Optimal conformations showing the possible proton transfer (*pro*-R H1) from C1 to O1. The process starts from the zwitterionic intermediate to the *cis*-enediol intermediate through a transition state, with relative energies shown in parentheses.

ZnOH configuration especially favors the channeling of thermal energy into the proton-transfer reaction.[55] Although the presence of Tyr152 makes the transfer of *pro*-R H1 as a proton unfavorable energetically, this hydrogen transfer may get a chance once the dynamical deviation of the aromatic ring of Tyr152 from its position stacking over the *pro*-R H1 takes place. In **zwitterion**, the negatively charged O1, as a strong proton acceptor, may promote the proton transfer from C1 to O1. Since the formation of a zwitterionic intermediate is quite facile and the zero-point energy and proton tunneling may lower the barrier by 2−3 kcal/mol, such proton transfer (*pro*-R H1) from C1 to O1 is likely to occur. Accordingly, at the stage of the zwitterionic intermediate, hydride transfer from C1 to C2 will result in the product G6P, while proton transfer from C1 to O1 may result in hydrogen exchange between substrate and solvent. Although the elucidation of the hydrogen exchange mechanism requires further experimental and theoretical investigations, the proposed zwitterionic intermediate provides one possibility to reconcile the hydride-shift and the *cis*-enediol intermediate mechanisms.

(55) Suárez, D.; Merz, K. M., Jr *J. Am. Chem. Soc.* **2001**, *123*, 3759. Smedarchina, Z.; Siebrand, W.; Fernández-Ramos, A.; Cui, Q. *J. Am. Chem. Soc.* **2003**, *125*, 243.

Conclusion

We have performed detailed QM(B3LYP)/MM stationary-point optimizations and extensive QM(PM3)/MM molecular dynamics simulations on the reversible isomerization of F6P to G6P catalyzed by *Pf*PGI. On the basis of the calculations and simulations, we proposed a zwitterionic intermediate mechanism for the low-energy enzymatic reaction, involving both proton and hydride transfers. Of significant interest, we found that the presence of the zwitterionic intermediate in the reaction can reconcile distinct mechanisms suggested in previous studies. Once the zwitterionic intermediate is formed, two types of hydrogen transfer may occur: the hydride transfer from C1 to C2, mediated by Tyr152, yields G6P, and the reversible proton transfer from C1 to O1, with the involvement of Zn^{2+}, accomplishes hydrogen exchange between substrate and solvent. At the QM(B3LYP)/MM level, the predicted low barriers for the proton/hydride transfers show that the overall enzymatic reaction is facile.

Whereas residues Glu97 and His158, as the general acid/base, catalyze proton transfer between the substrate and surrounding residues, calculations and simulations on mutants clarify the key roles of other conserved residues. Specifically, Tyr152 promotes the hydride transfer between C1 and C2, which is a rate-determining step. The conserved residues Tyr99, Tyr52, Tyr160, Thr71, Thr85, and Gly87, located at the bottom of the active pocket, constitute the hydrogen-bond network to the substrate, and they are responsible for the critical near-attack reactive conformation effect. Although Zn^{2+} was not directly involved in the isomerization reaction, the metal ion, as a structural anchor, constructs a hydrogen bond wire to connect the substrate to outer solvent molecules and residues, which may be a potential channel for the hydrogen exchange.

Acknowledgment. This work was supported by the National Science Foundation of China (20673087, 20733002, 20473062, 20423002) and the Ministry of Science and Technology (2004CB719902).

Supporting Information Available: Comparison of selected crystal structures, MM MD, QM/MM optimized configurations, highlight of the active sites, detailed data from the thermodynamic integrations for the whole reaction, and complete refs 34, 38, and 50. This material is available free of charge via the Internet at http://pubs.acs.org.

JA710633C